Marine Geology 319–322 (2012) 21–34

Contents lists available at SciVerse ScienceDirect

Marine Geology

journal homepage: www.elsevier.com/locate/margeo

Nd, Sr isotopes and elemental geochemistry of surface sediments from the South China Sea: Implications for Provenance Tracing

Gangjian Wei [a,*], Ying Liu [a], Jinlong Ma [a], Luhua Xie [b], Jianfang Chen [c], Wenfeng Deng [a], Song Tang [b]

[a] State Key Laboratory of Isotope Geochemistry, Guangzhou Institute of Geochemistry, Chinese Academy of Sciences, Guangzhou 510640, China
[b] Key Laboratory of Marginal Sea Geology, Guangzhou Institute of Geochemistry, Chinese Academy of Sciences, Guangzhou 510640, China
[c] The Second Institute of Oceanography, SOA, Hangzhou, China

ARTICLE INFO

Article history:
Received 10 August 2011
Received in revised form 29 February 2012
Accepted 28 May 2012
Available online 2 July 2012

Communicated by G.J. de Lange

Keywords:
sediment provenance
minerals
major and trace elements
Nd and Sr isotopes
South China Sea

ABSTRACT

The mineralogy, major and trace elements, and neodymium and strontium isotopes of surface sediments in the South China Sea (SCS) are documented with the aim of investigating their applicability in provenance tracing. The results indicate that mineralogical compositions alone do not clearly identify the sources for the bulk sediments in the SCS. The Nd isotopic compositions of the SCS sediments show a clear zonal distribution. The most negative ε_{Nd} values were obtained for sediments from offshore South China (−13.0 to −10.7), while those from offshore Indochina are slightly more positive (−10.7 to −9.4). The Nd isotopic compositions of the sediments from offshore Borneo are even higher, with ε_{Nd} ranging from −8.8 to −7.0, and the sediments offshore from the southern Philippine Arc have the most positive ε_{Nd} values, from −3.7 to +5.3. This zonal distribution in ε_{Nd} is in good agreement with the Nd isotopic compositions of the sediments supplied by river systems that drain into the corresponding regions, indicating that Nd isotopic compositions are an adequate proxy for provenance tracing of SCS sediments. Sr isotopic compositions, in contrast, can only be used to identify the sediments from offshore South China and offshore from the southern Philippine Arc, as the $^{87}Sr/^{86}Sr$ ratios of sediments from other regions overlapped. Similar zonal distributions are also apparent in a La–Th–Sc discrimination diagram. Sediments from the west margin of the SCS, such as those from Beibuwan Bay, offshore from Hainan Island, offshore from Indochina, and from the Sunda Shelf plot in the same field, while those offshore from the northeastern SCS, offshore from Borneo, and offshore from the southern Philippine Arc plot in distinct fields. Thus, the La–Th–Sc discrimination diagram, coupled with Nd isotopes, can be used to trace the provenance of SCS sediments. Using this method, we re-assessed the provenance changes of sediments at Ocean Drilling Program (ODP) Site 1148 since the late Oligocene. The results indicate that sediments deposited after 23.8 Ma (above 455 mcd: meters composite depth) were supplied mainly from the eastern South China Block, with a negligible contribution from the interior of the South China Block. Sediments deposited before 26 Ma (beneath 477 mcd) were supplied mainly from the North Palawan Continental Terrane, which may retain the geochemical characteristics of the materials covered on the late Mesozoic granitoids along the coastal South China. For that the North Palawan Continental Terrane is presently located within the southern Philippine Arc but was located close to ODP Site 1148 in the late Oligocene. The weathering products of volcanic material associated with the extension of the SCS ocean crust also contributed to these sediments. The rapid change in sediment source at 26–23.8 Ma probably resulted from a sudden cessation of sediment supply from the North Palawan Continental Terrane. We suggest that the North Palawan Continental Terrane drifted southwards along with the extension of the SCS ocean crust during that time, and when the basin was large enough, the supply of sediment from the south to ODP Site 1148 at the north slope may have ceased.

1. Introduction

The provenance of sediments and sedimentary rocks is an important component of the paleoceanography and tectonic history of a region. Geochemical methods have generally been used in tracing the provenance of sediments and sedimentary rocks, along with analyses of accessory detrital minerals, in particular the U–Pb geochronology of detrital zircon (Fedo et al., 2003 and references therein). In the absence of detrital zircon, elemental and isotopic geochemical methods are powerful tools in identifying provenance (McLennan et al., 1993), including analyses of rare earth elements (REEs) (Bhatia, 1985; McLennan, 1989) and immobile elements (Bhatia and Crook, 1986; Fralick and Kronberg, 1997). Sm–Nd isotope systematics are generally unaltered during sedimentary processes (McCulloch and Wasserburg,

* Corresponding author at: 511 Kehua Rd., Guangzhou Institute of Geochemistry, CAS, Guangzhou, 510640, China. Tel.: +86 20 85290093; fax: +86 20 85290130.
E-mail address: gjwei@gig.ac.cn (G. Wei).

0025-3227/$ – see front matter © 2012 Elsevier B.V. All rights reserved.
doi:10.1016/j.margeo.2012.05.007

1978), meaning that Nd isotopes provide reliable evidence of provenance (Goldstein et al., 1984; Miller and O'Nions, 1984, 1985; Goldstein and Jacobsen, 1988). Previous studies have also investigated other isotopic systems, including Sr and Pb (McLennan et al., 1993; Vroon et al., 1995; Derry and France-Lanord, 1996; Graham et al., 1997; Winter et al., 1997). However, the complicated nature of sedimentary processes, and the fact that different components in sediments and sedimentary rocks may be derived from different sources, suggests that the use of a single geochemical method may not always be a reliable identifier of provenance; instead, several complementary geochemical methods should be employed (Fedo et al., 2003).

The South China Sea (SCS) is the largest marginal sea in the Western Pacific. The SCS oceanic crust emerged in the late Oligocene (~30 Ma) (Briais et al., 1993) and evolved in the context of Cenozoic tectonic activity in Southeast Asia and the Southwest Pacific (Hall, 2002). The sea–land distribution changed significantly during this period (Hall, 2002), indicating a change in the source of sediment supplied to the SCS. Therefore, an analysis of temporal trends in sediment provenance in this region may help to constrain its tectonic evolution.

One of the most significant changes in sediment provenance within the SCS occurred at around 23.8 Ma, as recorded in the sediment core recovered from ODP Site 1148 in the north basin of the SCS. At this time, the sedimentary Nd isotopes (ε_{Nd}) drifted by about 2 units (Clift et al., 2002; Li et al., 2003), coincident with significant changes in the assemblage of clay minerals (Clift et al., 2002; Tang et al., 2004), elemental compositions (Li et al., 2003), and the physical and other characteristics of the sediment (Wang et al., 2000; Li et al., 2005). A sediment core recovered from the Pearl River Mouth Basin in the northern SCS also shows a significant ε_{Nd} drift at this time (Shao et al., 2008). A similar negative ε_{Nd} drift has been reported in sediment core recovered from the Yinggehai-Song Hong and Qiongdongnan Basins in the northwest SCS, although this occurred much later, at around 13.8 Ma (Yan et al., 2007), while in the sediments from Hanoi Basin supplied by the Red River systems, there exists a significant positive ε_{Nd} drift at around 24 Ma (Clift et al., 2006a).

The interpretation of these provenance changes is a matter of debate. One explanation is the progressive headward erosion of river systems in South China, from the coastal South China region prior to 23.8 Ma, to the interior of the South China Block after 23.8 Ma (Clift et al., 2002; Shao et al., 2008). In contrast, Li et al. (2003) suggested that sediment input from the southern SCS to ODP Site 1148 ceased at 23.8 Ma, related to the progressive enlargement of the SCS. The interpretation of these changes in provenance is important because it has implications for tectonic reconstructions of the region.

This debate could be resolved by examining provenance information from geochemical proxies, in particular Nd isotopes, which are commonly used to trace the provenance of sediments and sedimentary rocks (Clift et al., 2002; Li et al., 2003; Yan et al., 2007; Shao et al., 2008, 2009). However, the applicability and limitations of Nd isotopes are not yet fully understood. Some studies have compared the Nd isotopes of sediments with those of potential source rocks (e.g., Clift et al., 2002); however, intensive chemical weathering can cause significant Nd isotope fractionation, with ε_{Nd} drifts of up to 2.5 units in secondary minerals of weathering products compared with the parent rock (Ma et al., 2010). Therefore, the mineral compositions of sediments, in particular the proportion of clay minerals (secondary minerals) and rock-forming minerals (primary minerals), should be considered when employing Nd isotopes for provenance analysis, and care should be taken to identify ε_{Nd} drifts related to chemical weathering.

The applicability and limitations of geochemical methods for tracing the provenance of SCS sediments can be assessed by analyzing the geochemical composition of surface sediments compared with that of potential source rocks. The current continent-island–sea distribution in this region was established by the late Pliocene (Hall, 2002), and the pattern of sediment supply can be roughly constrained. The Philippine island arcs form the eastern boundary of the SCS, dominated by young volcanic rocks, mainly basalt and andesite. The isotopic and elemental compositions in this region are different from those in South China and Indochina, to the north and west of the SCS, respectively (Chen et al., 1990; McDermott et al., 1993, 2005). Moreover, previous studies have reported the Nd isotopes of sediments and suspended particles in some of the main river systems around the SCS (Chen and Lee, 1990; Liu et al., 2007; Shao et al., 2009). This information is important in constraining the geochemical composition of the possible sources of SCS sediments, and in linking the sediments to potential source rocks.

Previous studies have investigated the provenance of sediments in the SCS. For example, Shi et al. (2007) examined mineral suites to identify sediment provenance around the Zhongsha Islands (Macclesfield Bank) in the northern SCS, and Liu et al. (2008) examined the assemblage of clay minerals within the fine-grained component of SCS sediments. Element discrimination diagrams has been used to identify the provenance of sediments around the Pearl River Mouth region (Yang et al., 2008), and Gui et al. (1994) mapped the distribution of strontium and oxygen isotopes in the silicate fraction of sediments from the southern SCS. In addition, the Nd isotopes of surface sediments have been used to distinguish between northern and southern provenances for sediments in the SCS (Li et al., 2003). However, few studies have integrated mineralogical, elemental, and isotopic geochemical data to investigate the provenance of sediments in the SCS. As a result, some of the key linkages relevant to provenance tracing remain poorly understood. For example, what is the relationship between the geochemical composition of SCS sediments and that of potential sources? And to what extent can these geochemical methods be used to identify the provenance of SCS sediments? It is important to answer these questions if we wish to assess the applicability of these geochemical methods in tracing the provenance of sediments in the SCS.

This study examines the mineralogy, major and trace elements, and neodymium and strontium isotopes of surface sediments throughout the SCS, with the aim of investigating their applicability in provenance tracing. The geochemical composition of sediments, which may provide provenance information, is discussed in terms of its spatial distribution, and we examine the relationship between the geochemical composition of sediments in different regions and potential sources, with a view to provenance tracing. The results contribute to our understanding of the geochemical linkage between the sediments and their sources, and to the application of these geochemical methods in provenance tracing. Based on the findings, we re-assess the significance of provenance changes recorded in sediments from ODP Site 1148 since the late Oligocene.

2. Materials and methods

Thirty-four core-top sediments in the SCS were selected for analysis. The locations of the samples are listed in Table 1. The sediments are silty clay or clay, as well as foraminifer shells.

The samples were first reacted with 2N of acetic acid (HAc) to remove biogenic carbonates. The solid material was then collected by centrifugation, oven-dried at 100 °C, and ground to powder for elemental, isotopic and mineral geochemical analysis.

The sample powders for analyses of major and trace elements, and Sr and Nd isotopes were first heated at 700 °C to destroy organic material. They were then digested by an $HNO_3 + HF$ acid mixture in high-pressure bombs for elemental analysis. Major elements were measured on a Varian Vista Pro inductively coupled plasma atomic emission spectrometer (ICP-AES) at the State Key Laboratory of Isotope Geochemistry, Guangzhou Institute of Geochemistry (GIG), Chinese Academy of Sciences (CAS). Trace elements were measured on a Perkin-Elmer Elan 6000 inductively coupled plasma mass spectrometer (ICP-MS) at the same laboratory. The analyses of major and trace

Table 1
Locations and major elements of the sediments (unit: %).

Sample ID	Locations	Al_2O_3	CaO	FeO(T)	K_2O	MgO	MnO	Na_2O	P_2O_5	TiO_2
Beibuwan Bay										
B22	20°36′00″N, 108°05′00″E	5.80	0.12	3.79	1.09	0.89	0.03	0.46	0.05	0.55
B36	20°22′00″N, 109°30′00″E	11.01	0.27	5.43	2.18	1.49	0.06	0.99	0.06	0.95
B39	20°08′00″N, 108°20′00″E	9.36	0.26	5.44	2.15	2.28	0.05	1.01	0.04	0.72
B55	19°40′00″N, 107°52′00″E	7.84	0.40	3.29	1.90	1.25	0.04	1.06	0.04	0.64
B61	19°30′00″N, 107°10′00″E	15.31	0.33	7.00	2.74	2.26	0.08	1.22	0.09	1.15
B78	18°58′00″N, 107°52′00″E	12.14	0.39	4.16	2.68	1.80	0.05	1.36	0.05	0.90
Offshore Hainan Island										
S003	20°00′00″N, 112°00′00″E	8.18	0.35	2.02	2.10	0.74	0.04	1.30	0.04	0.64
S009	18°00′00″N, 110°00′00″E	6.03	0.28	2.08	1.79	0.58	0.03	0.79	0.04	0.64
Northwest Basin										
S007	18°00′00″N, 114°00′00″E	14.60	1.34	5.44	3.40	1.95	0.80	1.96	0.11	1.05
Offshore Indochina										
S013	16°00′00″N, 110°00′00″E	13.24	0.77	5.08	3.17	1.61	0.22	1.84	0.12	1.20
S016	15°00′00″N, 110°30′00″E	12.74	0.70	3.97	3.27	1.18	0.27	1.54	0.10	1.31
S029	11°00′00″N, 110°00′00″E	16.22	2.23	6.73	2.79	2.07	0.06	1.80	0.19	0.83
NS90-68	8°22′13″N, 107°22′58″E	8.47	1.54	3.31	1.59	1.37	0.05	0.75	0.09	0.59
NS90-70	8°52′01″N, 108°39′54″E	4.16	0.20	1.65	1.46	0.31	0.02	0.80	0.03	0.20
Southwest Basin and Nansha Islands										
S018	15°00′00″N, 111°30′00″E	17.24	1.76	6.88	2.69	1.86	0.95	1.38	0.20	0.80
S021	14°00′00″N, 113°00′00″E	14.26	1.81	6.26	3.24	1.91	1.14	2.04	0.19	0.92
S024	12°00′00″N, 112°00′00″E	15.49	0.28	5.60	3.00	1.92	0.75	1.31	0.05	0.94
S031	10°30′00″N, 111°00′00″E	13.76	2.69	5.06	3.19	2.13	2.37	1.30	0.09	0.97
S033	10°00′00″N, 112°00′00″E	14.73	2.32	7.88	3.24	2.26	2.74	1.25	0.20	0.92
S035	9°30′00″N, 113°00′00″E	9.10	2.03	3.27	2.39	0.95	2.40	1.29	0.17	1.00
S043	7°30′00″N, 111°00′00″E	13.53	2.60	4.98	3.28	2.14	2.35	1.08	0.10	1.07
S047	7°15′00″N, 113°00′00″E	14.52	3.04	6.66	3.44	2.71	3.03	1.11	0.19	1.07
S057	11°00′00″N, 115°00′00″E	7.89	28.75	2.71	0.75	0.50	0.15	0.86	0.21	0.27
Offshore Borneo										
S052	7°15′00″N, 115°30′00″E	10.24	1.28	6.29	1.54	1.25	0.19	1.63	0.21	0.82
S053	7°30′00″N, 116°00′00″E	11.80	1.70	4.96	2.26	1.81	0.06	1.13	0.18	0.73
NS88-44	5°49′04″N, 114°39′04″E	8.46	0.39	3.73	2.22	1.56	0.05	1.36	0.05	0.81
NS88-62	4°24′13″N, 113°20′10″E	15.15	1.30	5.78	2.88	2.58	0.07	1.11	0.13	0.87
NS88-68	4°33′58″N, 113° 5′50″E	10.24	1.28	6.29	1.54	1.25	0.19	1.63	0.21	0.82
Sunda Shelf										
NS89-61	4°04′21″N, 109°03′58″E	6.25	0.86	3.37	2.23	0.86	0.03	1.24	0.04	0.39
NS90-40	6°08′10 ″N, 108°37′40″E	6.13	0.27	3.46	1.71	1.03	0.07	0.94	0.04	0.39
NS90-54	6°51′13″N, 107°09′34″E	5.68	1.58	2.14	1.10	1.11	0.04	0.61	0.07	0.37
NS90-57	5°20′02″N, 106°52′32″E	3.52	0.16	2.44	1.01	0.59	0.04	0.59	0.03	0.23
NS90-59	4°33′31″N, 105°17′05″E	13.95	5.30	5.82	2.61	2.62	0.11	1.85	0.19	1.08
Northeast Basin										
92	19°33′54″N, 120°09′18″E	18.52	0.21	5.62	3.58	1.50	0.14	1.77	0.07	1.05
94	19°17′30″N, 118°31′48″E	15.27	0.63	5.95	2.69	1.85	3.35	2.06	0.10	0.92
105	18°54′18″N, 119°42′35″E	16.12	0.59	5.91	2.82	1.89	0.14	2.20	0.05	0.96
165	18°20′24″N, 117°32′00″E	15.57	0.58	5.80	2.79	2.02	0.27	2.06	0.06	0.90
185	17°00′42″N, 117°49′36″E	17.55	0.66	6.52	3.27	2.26	0.44	2.23	0.07	1.01
Offshore southern Philippine Arc										
198	16°10′36″N, 118°40′12″E	14.68	2.23	5.21	2.11	2.18	0.36	3.43	0.07	0.61
208	15°54′06″N, 118°40′00″E	14.07	2.31	5.30	2.09	2.01	0.47	3.60	0.08	0.62
254	14°29′30″N, 118°59′42″E	15.82	3.81	3.25	2.14	2.13	0.09	5.35	0.04	0.36
295	13°12′18″N, 118°23′00″E	13.61	4.38	5.29	2.33	1.86	1.32	3.42	0.14	0.80
307	12°39′00″N, 117°01′48″E	12.07	3.09	4.32	2.25	2.03	0.33	2.07	0.10	0.74
320	13°23′48″N, 118°23′30″E	11.50	4.03	6.29	1.89	1.85	3.25	2.24	0.30	0.70

elements followed the methods described by Liu et al. (1996) and Li et al. (2002), respectively. The precision for major elements was better than 1% (Li et al., 2002), and for trace elements was generally better than 5% (Liu et al., 1996). The results of analyses of major and trace elements are presented in Tables 1 and 2, respectively. Several USGS and Chinese soil and sediment standard references (for soil: GSS-5, GSS-7, and GXR-6; for sediment: GSD-9 and GSD-12) were repeatedly measured with the samples, yielding values that were generally within ±2% and ±10% (RSD) of the certified values for major and trace elements, respectively. The major and trace elements of sediments from offshore Indochina, offshore Borneo and from the Sunda Shelf in the southern SCS were also analyzed using the same methods, and the results were included in Tables 1 and 2, along with their Nd isotopes, as measured by Li et al. (2003).

The samples for Sr–Nd isotopic analysis were also digested using an HNO_3 + HF mixture, and finally dissolved in a 2N HCl solution. The sample solution was then loaded into a column filled with AG50-X8 cation resin. Both Sr and REEs were trapped on the column. The column was rinsed with 2N of HCl eluant. Sr and REEs were de-trapped from the column using 2N and 3N HCl, respectively. The

Table 2
Trace elements (in ppm) and Nd, Sr isotopes of the sediments.

Sample ID	B22	B36	B39	B55	B61	B78	S003	S009
Sc	5.30	10.2	8.65	6.29	15.3	10.9	5.82	4.38
V	72.2	108	102	59.5	121	88.4	47.9	45.5
Cr	26.1	57.2	53.7	51.1	82.4	62.9	29.2	19.5
Co	6.10	10.8	10.1	6.69	14.3	8.77	4.29	4.07
Ni	12.2	21.4	19.3	14.4	38.4	20.6	9.47	7.03
Cu	14.2	22.0	17.1	11.4	29.5	17.8	7.84	8.58
Zn	17.8	44.9	39.3	39.3	88.8	61.8	31.7	27.6
Ga	10.0	17.0	14.9	11.4	24.1	17.3	11.0	8.75
Ge	1.36	1.79	1.81	1.35	2.33	1.99	1.41	
Rb	68.0	123	117	90.7	161	142	108	84.6
Sr	36.3	66.4	66.9	84.0	75.5	87.3	82.7	65.7
Y	11.3	18.4	14.1	13.4	21.2	21.3	15.9	12.5
Zr	79.2	127	94.0	75.2	147	123	92.3	95.9
Nb	12.6	20.3	16.5	14.9	23.7	19.5	14.2	14.8
Cs	5.96	10.3	9.05	5.62	14.0	11.5	5.89	4.41
Ba	187	385	349	352	430	447	377	279
La	14.0	29.2	21.1	21.4	37.4	27.0	23.5	26.5
Ce	35.4	69.3	48.7	45.7	85.3	62.1	52.1	61.1
Pr	3.29	6.89	4.95	4.75	8.53	6.26	5.35	6.33
Nd	13.1	27.2	19.2	18.3	32.1	23.3	20.1	23.7
Sm	2.44	4.95	3.24	3.11	5.44	4.01	3.55	4.00
Eu	0.43	0.85	0.55	0.55	0.97	0.71	0.61	0.62
Gd	1.88	3.70	2.53	2.16	4.09	3.18	2.61	2.66
Tb	0.31	0.64	0.43	0.39	0.66	0.54	0.45	0.42
Dy	1.96	3.69	2.57	2.34	3.89	3.36	2.73	2.25
Ho	0.40	0.72	0.52	0.46	0.77	0.70	0.56	0.42
Er	1.15	2.17	1.57	1.39	2.34	2.03	1.64	1.29
Tm	0.20	0.32	0.25	0.22	0.37	0.33	0.27	0.20
Yb	1.14	2.00	1.56	1.43	2.37	2.03	1.66	1.16
Lu	0.19	0.31	0.24	0.22	0.37	0.32	0.26	0.19
Hf	2.11	3.37	2.68	2.14	3.86	3.46	2.62	2.05
Ta	1.19	1.95	1.39	1.19	2.09	1.53	1.19	1.25
Pb	13.1	19.5	20.1	18.3	25.3	16.9	14.2	13.0
Th	8.59	17.16	12.36	8.30	20.9	12.6	9.29	11.0
U	1.61	2.96	2.19	1.72	3.63	2.58	1.81	1.60
Eu^*	0.70	0.68	0.66	0.71	0.73	0.68	0.69	0.67
$^{87}Sr/^{86}Sr$	0.731040 ± 18	0.727645 ± 17	0.725148 ± 19	0.720986 ± 13	0.727262 ± 19	0.724148 ± 19	0.723583 ± 19	0.724684 ± 19
$^{143}Nd/^{144}Nd$	0.512088 ± 12	0.512087 ± 10	0.512064 ± 12	0.512059 ± 12	0.512117 ± 12	0.512056 ± 12	0.512043 ± 12	0.512035 ± 12
ε_{Nd}	−10.73	−10.75	−11.20	−11.30	−10.17	−11.35	−11.61	−11.76

S007	S013	S016	S018	S029	NS90-68#	NS90-70#	S021	S024
13.7	12.7	13.1	17.9	15.4	8.32	2.49	13.9	15.0
113	155	150	128	108	62.4	18.8	135	129
72.0	72.2	65.3	72.6	78.8	47.7	15.1	69.1	85.2
16.3	11.7	9.80	20.2	13.1	6.92	2.30	16.3	15.5
75.8	40.2	38.1	111	43.9	22.3	4.55	122	56.9
57.3	23.3	21.8	47.1	30.2	10.3	4.11	63.0	59.9
97.9	89.2	90.5	146	104	41.9	17.1	123	92.0
22.1	20.9	20.1	25.6	21.7	10.9	4.21	26.9	23.2
2.72	2.79	3.38	2.25	1.97	1.30	1.28	2.65	2.57
160	155	161	144	137	77.5	53.6	157	163
126	109	102	155	163	114	45.0	174	75.1
19.5	25.1	22.1	23.3	23.6	16.0	6.9	18.7	16.9
147	186	184	121	135	94.8	51.4	129	140
20.5	24.6	26.6	16.6	17.9	10.9	4.8	18.2	19.5
13.8	13.0	12.4	12.9	11.9	–	–	13.9	15.7
953	516	532	1101	501	167	241	1418	696
28.5	32.6	28.4	26.8	33.1	19.8	14.6	21.7	22.3
74.3	88.2	90.1	75.2	79.6	47.2	30.2	68.8	51.0
6.40	7.58	6.90	6.31	7.93	4.93	3.32	4.77	5.09
24.1	28.4	26.3	23.9	30.8	17.4	12.0	18.7	19.6
4.23	4.90	4.54	4.35	5.63	3.33	2.28	3.35	3.48
0.70	0.89	0.82	0.77	1.08	0.64	0.42	0.51	0.62
3.19	3.94	3.65	3.79	4.50	2.91	1.65	2.90	2.88
0.56	0.73	0.61	0.63	0.78	0.50	0.25	0.47	0.48
3.44	4.40	3.87	3.76	4.49	2.90	1.36	3.09	3.04
0.72	0.90	0.81	0.75	0.87	0.60	0.27	0.64	0.61
2.18	2.69	2.62	2.37	2.66	1.74	0.73	1.96	1.87
0.36	0.43	0.41	0.37	0.40	0.27	0.11	0.31	0.31
2.36	2.67	2.67	2.27	2.58	1.79	0.78	2.09	2.03
0.37	0.41	0.43	0.35	0.39	0.27	0.12	0.32	0.34
3.75	4.46	4.65	3.13	3.31	2.42	0.87	3.44	4.06
1.69	2.22	2.21	1.32	1.41	0.88	0.43	1.39	1.84
23.3	18.6	21.3	32.3	30.2	13.1	7.1	34.3	17.0
17.8	18.4	20.8	17.8	17.2	9.91	5.00	17.1	12.6

Table 2 (*continued*)

Sample ID	B22	B36	B39	B55	B61	B78	S003	S009
2.66	3.17	3.36	2.64	4.65	2.09	0.89	2.56	2.66
0.64	0.66	0.70	0.66	0.72	0.69	0.77	0.57	0.67
0.718058 ± 18	0.720548 ± 17	0.717267 ± 17	0.715053 ± 17	0.715303 ± 17	0.722726 ± 30	–	0.713366 ± 9	0.726755 ± 20
0.512074 ± 12	0.512046 ± 12	0.512100 ± 12	0.512081 ± 12	0.512097 ± 12	0.512102 ± 9	0.512155 ± 7	0.512162 ± 12	0.512105 ± 12
−11.00	−11.55	−10.49	−10.87	−10.55	−10.46	−9.42	−9.29	−10.41
S031	S033	S035	S043	S047	S052	S053	NS88-44#	NS88-62#
15.8	17.3	10.2	13.5	15.1	12.7	13.2	12.3	6.74
132	151	157	155	161	136	118	98.8	47.8
77.9	79.4	40.2	68.4	77.3	70.1	169	68.0	61.3
16.8	22.1	15.4	16.1	19.5	12.7	11.1	9.08	7.70
88.5	164	146	76.7	107	89.9	74.2	34.0	16.3
46.2	64.6	50.3	39.0	38.5	28.6	29.0	17.8	131
149	128	169	134	148	75.2	71.7	58.5	50.1
25.4	31.8	17.9	23.8	26.7	19.5	19.1	16.0	9.8
3.77	3.12	2.75	3.54	3.37	3.42	1.55	1.96	2.90
175	168	124	175	178	152	77.7	109	90.9
88.3	154	228	84.4	99.2	92.2	219	162	79.8
23.7	21.6	18.5	22.7	21.2	22.1	18.6	19.4	21.3
162	140	184	168	165	158	118	111	107
21.6	18.8	20.3	22.4	21.0	17.4	14.7	12.9	21.4
16.7	15.5	8.64	15.9	17.2	14.2	7.49	-	-
710	1543	1824	612	894	769	661	182	352
22.5	23.3	17.4	20.3	22.6	15.0	15.1	23.7	48.8
69.9	75.8	81.6	67.3	70.0	59.1	58.8	60.7	100
5.16	5.31	4.21	4.61	5.10	3.50	3.73	5.89	11.67
19.8	20.3	15.9	18.1	19.7	13.5	14.7	21.1	41.5
3.67	3.63	2.85	3.26	3.50	2.45	2.68	4.03	7.16
0.66	0.56	0.36	0.59	0.58	0.44	0.50	0.78	1.02
3.50	3.31	2.78	3.27	3.07	2.40	2.42	3.40	5.46
0.58	0.57	0.44	0.58	0.54	0.47	0.43	0.58	0.84
3.61	3.63	3.04	3.75	3.43	3.43	2.91	3.46	4.29
0.76	0.75	0.65	0.79	0.72	0.76	0.62	0.73	0.82
2.44	2.30	2.02	2.53	2.41	2.49	1.97	2.18	2.39
0.41	0.36	0.33	0.40	0.38	0.43	0.32	0.33	0.37
2.67	2.33	2.10	2.72	2.53	2.95	2.05	2.17	2.43
0.41	0.37	0.35	0.43	0.40	0.45	0.32	0.35	0.38
3.93	3.70	4.08	4.26	3.99	4.42	3.20	2.92	3.15
1.82	1.44	1.55	1.73	1.59	1.35	1.07	1.05	1.70
15.7	36.8	54.1	16.5	27.2	14.6	26.2	18.1	13.3
17.2	19.9	19.5	18.3	19.1	12.7	12.9	13.5	20.7
4.58	2.78	2.68	3.02	2.97	3.15	3.02	2.91	3.13
0.63	0.55	0.45	0.60	0.59	0.56	0.66	0.72	0.59
0.724758 ± 17	0.715740 ± 19	0.712441 ± 16	0.725279 ± 17	0.720711 ± 17	0.717031 ± 13	0.709882 ± 17	0.715360 ± 56	0.720602 ± 18
0.512080 ± 13	0.512059 ± 11	0.512110 ± 12	0.512063 ± 12	0.512127 ± 12	0.512216 ± 11	0.512282 ± 12	0.512200 ± 8	0.512189 ± 7
−10.88	−11.30	−10.30	−11.21	−9.96	−8.23	−6.95	−8.54	−8.76
NS88-68#	NS90-40#	NS90-54#	NS90-57#	NS90-59#	NS89-61#	S057	92	94
15.1	5.38	5.18	2.78	13.9	4.55	8.06	16.1	16.9
118	36.7	37.3	23.8	96.4	31.7	51.1	141	149
81.3	28.0	31.8	22.0	89.7	58.7	7.47	85.1	68.5
11.3	7.45	4.77	3.67	14.2	5.76	14.2	9.06	28.4
38.5	14.6	14.6	7.1	40.4	16.5	20.8	22.6	128
18.2	20.1	9.5	31.0	29.6	44.6	65.7	43.3	88.9
66.6	36.4	28.8	18.0	90.8	34.6	80.6	62.2	166
20.2	6.9	7.2	4.0	18.7	6.9	10.4	23.3	24.6
2.14	1.59	0.87	1.07	2.49	2.55	0.12	2.50	2.42
143	66.9	54.6	40.0	128	85.3	34.8	170	127
127	60.2	96.4	33.9	370	99.4	1467	88.9	109
23.3	10.4	10.1	6.7	28.2	14.8	27.7	22.6	18.9
136	68.7	64.1	46.7	133	78.5	53.3	147	145
15.1	8.1	7.8	5.1	19.9	8.8	6.5	19.7	13.5
–	–	–	–	–	–	3.50	14.8	11.0
259	248	134	148	364	403	1568	550	785
27.3	14.1	15.2	13.2	41.3	30.5	24.2	27.0	21.3
67.3	35.6	34.6	31.6	87.7	66.9	38.1	56.7	52.2
6.70	3.54	3.78	3.21	10.31	7.45	5.37	5.99	4.82
23.6	12.7	13.5	11.3	36.6	26.1	22.5	22.6	18.7
4.15	2.42	2.50	2.07	6.82	4.85	4.49	3.82	3.16
0.81	0.50	0.46	0.37	1.31	0.65	0.86	0.66	0.63
3.64	2.19	2.09	1.71	6.03	3.98	4.56	2.73	2.69
0.62	0.35	0.35	0.25	0.99	0.57	0.72	0.49	0.48
3.79	1.96	1.90	1.30	5.39	3.07	4.09	3.26	2.92
0.79	0.40	0.38	0.26	1.03	0.58	0.83	0.66	0.62
2.35	1.12	1.05	0.71	2.98	1.60	2.47	2.05	1.96
0.37	0.17	0.17	0.11	0.44	0.24	0.36	0.34	0.33

(*continued on next page*)

Table 2 (*continued*)

Sample ID	B22	B36	B39	B55	B61	B78	S003	S009
2.55	1.12	1.09	0.69	2.86	1.57	2.24	2.44	2.06
0.40	0.17	0.16	0.11	0.45	0.24	0.36	0.34	0.32
3.74	1.45	1.25	0.81	3.30	2.39	1.24	3.70	3.17
1.28	0.65	0.61	0.40	1.85	0.74	0.43	1.46	0.97
20.1	9.31	7.44	5.22	29.0	13.7	42.4	17.3	19.1
14.7	7.01	7.09	5.12	19.4	13.9	7.15	13.0	10.8
3.50	1.23	1.40	0.83	4.09	2.56	1.81	2.55	1.92
0.71	0.76	0.69	0.72	0.71	0.55	0.67	0.68	0.72
0.719912 ± 17	0.714553 ± 14	0.720555 ± 30	0.719230 ± 17	0.721330 ± 40	0.720222 ± 28	0.709235 ± 17	0.719055 ± 13	0.713477 ± 17
0.512191 ± 7	0.512111 ± 7	0.512088 ± 8	0.512042 ± 6	0.512009 ± 10	0.512129 ± 8	0.512283 ± 11	0.512154 ± 13	0.512232 ± 13
−8.72	−10.28	−10.73	−11.63	−12.28	−9.93	−6.93	−9.44	−7.93
105	165	185	198	208	254	295	307	320
16.4	17.3	17.9	12.8	13.2	8.03	14.7	11.9	15.6
142	143	148	101	137	58.7	173	139	154
78.1	77.9	84.2	61.3	53.5	20.7	29.1	58.6	31.5
12.6	31.3	24.1	22.3	20.1	9.36	16.6	16.7	25.0
32.6	52.9	53.6	75.6	74.2	15.7	72.3	81.8	138
51.0	91.8	101	90.0	99.9	19.9	38.6	80.6	94.1
80.5	86.8	102	70.9	85.3	52.6	93.3	73.9	114
20.7	21.1	22.8	18.6	17.9	18.4	18.6	16.2	21.6
2.17	2.39	2.47	1.74	1.63	1.07	2.01	2.03	1.42
130	134	144	74.4	70.3	55.0	80.3	103	69.4
104	110	111	237	228	417	342	202	349
18.1	19.6	18.0	13.0	14.3	11.7	17.9	16.3	18.5
130	142	136	113	97.4	61.6	140	128	104
15.8	14.6	15.8	8.2	7.7	5.8	9.5	11.5	8.9
11.3	12.3	12.8	6.35	5.72	4.00	6.25	9.61	6.10
527	979	901	837	1059	510	1455	1752	2235
23.6	23.3	24.3	14.6	15.3	14.2	15.8	14.4	13.6
50.6	53.7	57.2	33.7	35.1	26.8	41.1	41.6	45.3
5.45	5.23	5.61	3.17	3.29	2.94	3.60	3.05	3.15
21.1	20.4	21.8	12.8	12.9	11.9	14.9	12.2	13.3
3.71	3.67	3.80	2.42	2.56	2.31	3.14	2.39	2.72
0.73	0.69	0.72	0.58	0.54	0.65	0.69	0.39	0.50
2.71	2.74	2.97	2.10	2.20	1.94	3.03	2.58	2.99
0.51	0.50	0.53	0.34	0.38	0.31	0.49	0.40	0.42
3.24	3.16	3.32	2.25	2.45	1.95	3.08	2.70	2.74
0.66	0.67	0.68	0.47	0.53	0.38	0.64	0.58	0.60
2.06	2.07	2.10	1.43	1.53	1.11	1.96	1.77	1.82
0.33	0.33	0.35	0.24	0.26	0.20	0.32	0.32	0.28
2.14	2.21	2.26	1.46	1.54	1.07	2.06	1.98	1.78
0.34	0.35	0.37	0.24	0.26	0.19	0.34	0.32	0.30
3.43	3.59	3.54	2.49	2.68	1.84	3.45	3.23	2.82
1.24	1.19	1.29	0.57	0.52	0.38	0.65	0.83	0.59
14.6	18.3	19.5	16.2	14.9	12.0	29.8	22.6	41.0
10.8	12.2	12.9	7.69	7.23	6.18	9.76	9.45	11.4
2.15	2.42	2.41	1.81	1.77	1.81	2.05	2.04	1.81
0.74	0.72	0.72	0.90	0.76	1.08	0.78	0.55	0.66
0.716697 ± 16	0.713764 ± 17	0.715510 ± 17	0.705755 ± 17	0.705773 ± 18	0.704326 ± 17	0.706674 ± 17	0.709025 ± 17	0.708098 ± 16
0.512103 ± 12	0.512215 ± 12	0.512140 ± 13	0.512554 ± 13	0.512598 ± 12	0.512909 ± 13	0.512668 ± 13	0.512476 ± 13	0.512586 ± 11
−10.43	−8.26	−9.72	−1.65	−0.79	5.29	0.59	−3.16	−1.02

$^{87}Sr/^{86}Sr$ of the NS series samples are from Gui et al. (1994), and their $^{143}Nd/^{144}Nd$ are from Li et al. (2003).
$Eu^* = 3Eu_N/(2Tb_N + Sm_N)$, where N indicates normalized to chondrite; $\varepsilon_{Nd} = 10000 \times (^{143}Nd/^{144}Nd/0.512638-1)$;
"–" indicates no measurement.

de-trapped REEs were further concentrated using an RE Spec column, and subsequently an LN Spec (HDEHP-based) column was used to separate Nd from REEs. For details of the column chemistry, see Wei et al. (2004).

Nd and Sr isotopic measurements were performed on a MicroMass Isoprobe multi-collector–inductively coupled plasma–mass spectrometer (MC–ICP–MS) at the State Key Laboratory of Isotope Geochemistry at GIG, CAS. $^{88}Sr/^{86}Sr = 0.1194$ was adopted to calibrate mass bias during the Sr isotope measurements, and the NBS SRM 987 standard was repeatedly measured with the samples to monitor the quality of the measurements, yielding an average $^{87}Sr/^{86}Sr$ of 0.710250 ± 10 (2σ) ($N = 10$). Mass bias during Nd isotope measurements was normalized using $^{146}Nd/^{144}Nd = 0.7219$. A standard Nd solution, JNdi-1, was repeatedly measured together with the samples, yielding a mean value of 0.512123 ± 8 (2σ) ($N = 10$) for $^{143}Nd/^{144}Nd$. For details of the method, see Wei et al. (2002) and Liang et al. (2003). The results of Sr and Nd isotope measurements are listed in Table 2.

Mineral compositions of the bulk sediments were measured on a Rigaku D/max-1200 diffractometer at GIG, CAS. X-ray diffraction (XRD) patterns of the samples were recorded between 1.5° and 70° (2 h) at a scanning speed of 2°/min with Cu/Kα radiation (30 mA and 40 kV). The results are listed in Table 3.

3. Results

The analyzed sediments are dominated by clay minerals and rock-forming minerals (quartz and feldspar). Illite is the main clay mineral, occurring in all the sediment samples at concentrations of 7.9%–46.0%. Smectite is only present in some of the samples, at contents of 2.6%–8.4%. The contents of quartz and feldspar range from 5% to 76% and from 6.1% to 62.1%, respectively. K feldspar and

Table 3
Mineralogical compositions of the sediments.

(unit: %)

Sample ID	Smectite	Illite	Quartz	K-feldspar	Albite	Ca-feldspar *	Pyroxene	Borgniezite	Hematite	Non-crystal#
Beibuwan Bay										
B22		17.9	76.0	4.3	1.8					
B36		26.0	55.4	9.3	9.3					
B39		25.7	57.7	10.1	6.5					
B55		14.8	68.7	6.2	10.3					
B61	8.4	25.0	41.7	12.3	12.6					
B78		30.0	49.7	7.4	10.9			2.0		
Offshore Hainan Island										
S003		12.9	50.1	7.7	29.3					
S009		7.9	65.7	18.3	8.1					
Northwest Basin										
S007	6.4	27.4	34.1	11.2	16.3		4.6			
Offshore Indochina										
S013	7.0	21.1	37.8	15.9	18.1					
S016	–	–	–	–	–	–	–	–	–	–
S029	2.6	19.6	47.3	9.8	20.7					
Southwest Basin & Nansha Islands										
S018	7.8	33.3	33.6	11.1	14.2					
S021	4.2	27.3	27.0	15.8	18.3					~10.0
S024		40.3	31.4	10.7	12.6					~5.0
S031		46.0	35.0	4.2	8.5		6.3			
S033	5.4	29.1	38.8	8.7	11.4		6.5			
S035	–	–	–	–	–	–	–	–	–	–
S043		38.9	37.9	7.3	9.2		6.7			
S047		34.4	38.2	8.6	10.5		8.3			
Offshore Berneo										
S052		28.0	39.4	9.0	12.2		11.5			
S053		17.7	54.9		22.1			5.3		
Northeast Basin										
92		39.4	42.9		15.7		2.0			
94		39.9	31		27.6				1.5	
105		34	39.9		24.5				1.6	
165	–	–	–	–	–	–	–	–	–	–
185		41.2	35.2		22.1				1.5	
Offshore southern Philippine Arc										
198		30.8	14.9			29.6		11.7		~13.0
208		19.8	14.4			34.6		16.2		~15.0
254		7.9	5			41.4		20.7		~25.0
295		13	21.8			40.5	8.2	6.5		~10.0
307		22.9	26.8			20.5	10.6		1.2	~18.0
320		26	18.1			40.9				~15.0

* Ca-feldspar contents are the mixture of Ca-feldspar, albite and K-feldspar because the spectrum is overlapped by those of the albite and K-feldspar.
# Abundances of the non-crystal are estimated.
"–" indicates no measurement.

albite are generally present, and Ca feldspar is observed in some of the sediments collected from close to the Philippine Arc (samples 198, 204, 254, 295, 307 and 320 in Table 3). Because the spectral peak of Ca feldspar overlaps with those of K feldspar and albite, the content of Ca feldspar, which ranges from 20.5% to 41.4%, includes all three of these feldspars. In addition to quartz and feldspar, pyroxene and borgniezite are observed in some of the sediments, with contents of 2.0%–11.5% and 2.0%–20.7%, respectively. Samples 94, 105, 185, and 307 contain 1.2%–1.6% hematite, and samples S021, S024, 198, 204, 254, 295, 307, and 320 contain an unknown non-crystalline material (5%–25%).

Because the sediments were digested by HF acid for major element analysis, their SiO_2 contents could not be determined. The contents of the other major elements show large variations. For examples, Al_2O_3 contents vary from 3.52% to 17.55%, and MnO contents from 0.03% to 3.35%. Sample S057 contains an anomalously high CaO content (28.75%), even after cleaning by HAc acid. The contents of trace elements also show large variations among the samples (Table 2).

$^{87}Sr/^{86}Sr$ ratios vary from 0.704326 ± 17 to 0.731040 ± 17, and $^{143}Nd/^{144}Nd$ ratios from 0.512009 ± 10 to 0.512909 ± 13, corresponding to a ε_{Nd} range from -12.28 to $+5.29$. High $^{143}Nd/^{144}Nd$ ratios are found mainly for samples from near the Philippine Arc, which generally have low $^{87}Sr/^{86}Sr$ ratios.

4. Discussion

4.1. Mineralogical compositions and implications for provenance

The clay mineral assemblage in SCS sediments has been proposed as a useful tool for tracing the provenance of the fine fraction (grain size <2 μm) (Liu et al., 2008). We analyzed bulk samples rather than the fine fraction, meaning that we cannot present a detailed analysis

of clay mineral assemblages. Illite is the main clay minerals in the studied sediments. Its abundance is generally negative correlated to that of quartz, except for those offshore from the southern Philippine Arc, in which both of the illite and quartz abundances are negative correlated to that of the Ca-feldspar. This suggests a dilution relationship, and appears not a provenance control. Moreover, illite is supplied by most of the river systems around the SCS (Liu et al., 2007, 2008); consequently, deciphering its provenance information could be difficult. In contrast, smectite is a potential provenance indicator in the SCS, because the main terrestrial smectite sources are concentrated around the Philippine Arc (Liu et al., 2008). However, smectite was not identified in the sediments near the Philippine Arc because its spectral peak overlaps with that of non-crystalline and unknown materials. Moreover, many samples from the western SCS contain smectite, far away from the Philippine Arc (e.g., samples S013, S018, S021, S029, and S033 from offshore Indochina, and sample B61 from Beibuwan Bay). This result indicates that the Philippine Arc is not the sole source of smectite in the region. The chemical weathering of volcanic rocks, in particular the weathering of basalt in seawater, may produce abundant smectite in addition to river-borne smectite in marine sediments (Thiry, 2000). In addition to the Philippine Arc, volcanic islands are found in many regions of the SCS. For example, some islands in Beibuwan Bay (e.g., Weizhou and Xieyan islands) are basalt, and Neogene basalts cover a large part of north Hainan Island and Leizhou Peninsula (Huang et al., 1993) and in the central and southern highlands of Vietnam (Barr and MacDonald, 1981). Chemical weathering of these volcanic rocks, under the influence of seawater, produce a large amount of smectite (>50%) in the weathering products (Ge, 2009). This source may provide much of the smectite in local sediments, thereby hindering a provenance determination based on smectite. Moreover, clay minerals generally account for less than 50% of the total sediment (Table 3). Thus, clay mineral assemblages may be an indicator of the provenance of clay minerals (Liu et al., 2008), but not of the bulk sediment in the SCS.

4.2. Provenance tracing using Nd and Sr isotopes

The ε_{Nd} values of these sediments, as well as the values reported by Li et al. (2003), are shown in Fig. 1. There are clear spatial variations in the Nd isotopes of sediments in the SCS. Sediments offshore from the southern Philippine Arc show the highest Nd isotope values; in particular, the ε_{Nd} values of sediments close to southern Luzon Island range from −3.7 to 5.3. The ε_{Nd} values of sediments offshore from Borneo are −7.0 to −8.8, and sediments located offshore from Indochina yield ε_{Nd} values of −10.9 to −9.4. More negative ε_{Nd} values are generally found in the northern SCS. In Beibuwan Bay, ε_{Nd} values are −11.3 to −10.7, and sediments offshore from Hainan Island yield values of −13.0 to −11.3. The ε_{Nd}

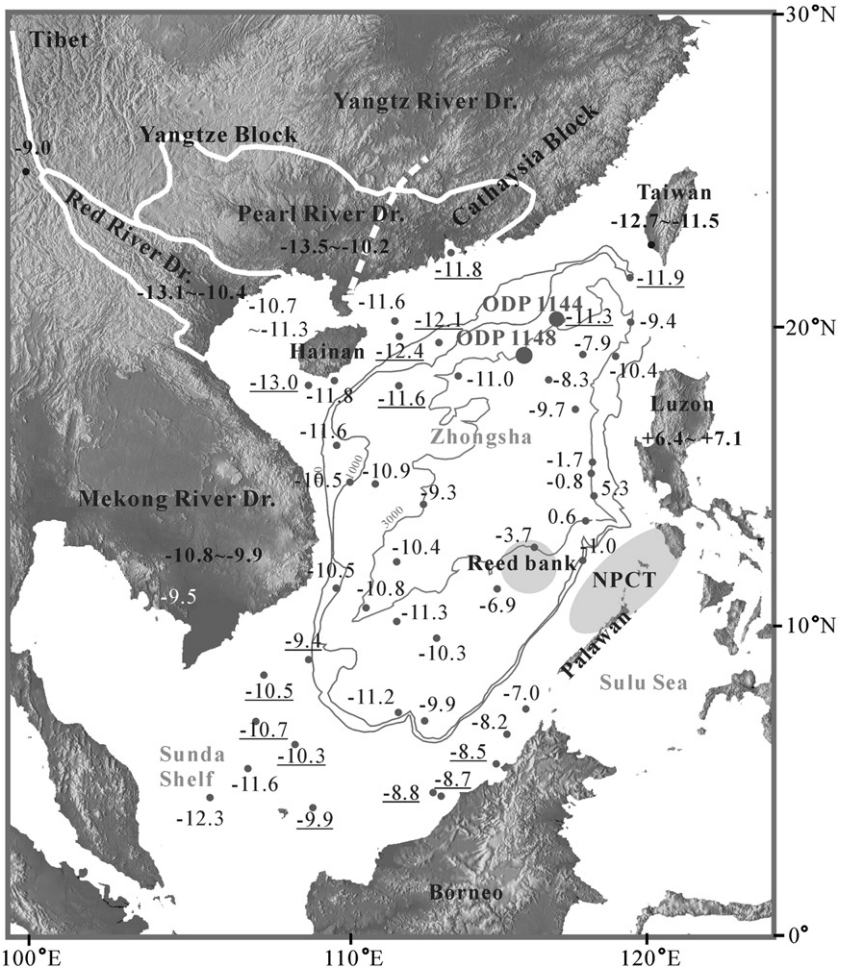

Fig. 1. Map showing the locations of the samples and their ε_{Nd} values. The underlined data are from Li et al. (2003). Thin lines show the 200, 1000, and 3000 m isobaths of the South China Sea. Bold dashed line shows the boundary between the Cathaysia Block and the Yangtze Block in South China according to Wang et al. (2003) and Zhang and Wang (2007). Shaded regions show the locations of the Reed Bank and the North Palawan Continental Terrane. The ε_{Nd} values of the suspended particles in the related river systems are also shown. Data of the Pearl River system are from Liu et al. (2008) and Shao et al. (2009); data of the streams on Taiwan Island are from Chen and Lee (1990) and Shao et al. (2009); data of the Red River systems are from Liu et al. (2008); data of the Mekong River system are from Goldstein et al. (1984), Liu et al. (2008), and Wu et al. (2010); and data of rivers in the Philippines are from Goldstein and Jacobsen (1988).

values of sediments from the eastern basin in the northern SCS vary from −11.9 to −11.3 (Fig. 1).

The distribution of ε_{Nd} values is consistent with the potential sources of terrestrial inputs from river systems drained to these regions. In the northern SCS, sediments are supplied mainly by the Red River, the Pearl River, and streams on the eastern South China Block and Taiwan Island. The ε_{Nd} values of the sediments in these river systems range from −13.1 to −10.4 (Red River), −13.5 to −10.2 (Pearl River), and −12.7 to −11.5 (eastern South China and Taiwan Island), respectively (Chen and Lee, 1990; Liu et al., 2008; Shao et al., 2009). These values are the most negative of those obtained for sediments of the northern SCS (Fig. 1).

It is worth noting that the ε_{Nd} values of the sediments supplied by these river systems in South China Block show some overlap, meaning it is difficult to identify the source river of Nd in the sediments based on ε_{Nd} alone. The South China Block comprises of two separate blocks, with the Cathaysia Block locating to the east and the Yangtze Block to the west. The southern boundary between these two blocks is located at Wuchuan–Sihui and Chenzhou–Linwu fault (also marked in Fig. 1) identified by significant changes in geochemical characteristics of the mafic rocks (Wang et al., 2003) and crustal structure (Zhang and Wang, 2007) across the fault. Thus, the sediments supplied from the east tributaries of the Pearl River, and streams at the coastal region of the eastern South China may have the geochemical characteristics of the Cathaysia Block. The main materials in the mountains in the west Taiwan Island are Cenozoic sediments, which may come from the eastern South China (Huang et al., 2006), thus sediments supplied from Taiwan Island may also have Cathaysia characteristics. In contrast, the main drainage of the Pearl River system is located in Yangtze Block. Even though its mouth is located in Cathaysia Block (Fig. 1), and the drainage of the Red River system is located in Yangtze Block and the northern edge of Indochina Block. Sediments supplied by these river systems, mainly distributing in the west of the north SCS, may have the geochemical characteristics of the Yangtze Block. However, the overlapped Nd isotopic values of these sediments indicate that using Nd isotopes alone could not identify the sources from the eastern South China Block (Cathaysia sources) and the western South China Block (Yangtze sources). Some other geochemical parameters should be adapted for such provenance tracing.

Sediments in the Mekong River system show slightly higher ε_{Nd} values than those of the South China Block, from −10.8 to −9.9 (Liu et al., 2008) or around −9.5 (Goldstein et al., 1984). This difference may be attributed to the contrasting geology of the South China Block and Indochina Block for that the Mekong River originates in the eastern Tibet Plateau, materials from the east Tibet Plateau may be carried by the Mekong River system (Clift et al., 2006b). The ε_{Nd} values of suspended particles in the upper reaches of the Mekong River are about −9.0 (Wu et al., 2010); i.e., higher than values obtained for the South China Block. In addition, there exist large amounts of Cenozoic basalt outcrops in the central and southern highlands of Vietnam, the lower reaches of the Mekong River systems (Barr and MacDonald, 1981), and basalt ε_{Nd} values are generally very positive. Input of such materials may account for the slightly more positive ε_{Nd} values in the sediments offshore from Indochina compared with those in the northern SCS.

Some stream sediments on Luzon Island have ε_{Nd} values ranging from +6.5 to +7.1 (Goldstein and Jacobsen, 1988). This region is dominated by volcanic rocks, such as basalt and andesite, that yields ε_{Nd} values ranging from −7 in the north to +8 in the south (Chen et al., 1990; McDermott et al., 1993, 2005). These rocks are likely to contribute to the high ε_{Nd} values of sediments offshore from the southern Philippine Arc (Fig. 1). There are no ε_{Nd} data from Borneo stream sediments or rocks; however, sediments offshore from Borneo show a narrow range of ε_{Nd} values (from −7.0 to −8.8), suggesting this is a characteristic value for sediments supplied from Borneo.

For sediments located away from these regions, mixing trends can be identified from Nd isotopes. For example, sediments in the northeast SCS basin yield ε_{Nd} values of −10.4 to −7.9, possibly indicating a mixture of sediments from the eastern South China (including Taiwan Island) and the Philippine Arc, while sediments from near the Nansha Islands (Spratley Islands) may be mixed with those from the southern Philippine Arc, Borneo, and the Indochina Block, as the ε_{Nd} values are intermediate between those of these three regions. The agreement between the ε_{Nd} values of sediment in the SCS and their possible sources indicates that Nd isotopes are reliable in tracing the provenance of SCS sediments.

Strontium isotope ratios are also a useful proxy for sediment provenance, especially for distinguishing basic rock provenances from typical continental sources (Asahara et al., 1999; Hemming et al., 2007). Gui et al. (1994) reported that sediments from the southern SCS show a significant spatial zoning in Sr isotopes, with low $^{87}Sr/^{86}Sr$ ratios offshore from the southern Philippine Arc and increasing towards the Sunda Shelf. Zonal $^{87}Sr/^{86}Sr$ distribution can also be seen in our results, with the lowest $^{87}Sr/^{86}Sr$ values in the sediments offshore from the southern Philippine Arc (0.704~0.709), and the highest in Beibuwan Bay. As coupling Sr and Nd isotopes is one of the mostly applied methods in geochemistry tracing, Fig. 2 shows the correlation between Sr and Nd isotopes. The sediments offshore from the southern Philippine Arc (SPA) have the highest $^{143}Nd/^{144}Nd$ ratios and the lowest $^{87}Sr/^{86}Sr$ ratios, while sediments from Beibuwan Bay and offshore from Hainan Island, which may represent the sediments from South China and labeled as SC, show the lowest $^{143}Nd/^{144}Nd$ ratios and highest $^{87}Sr/^{86}Sr$ ratios (Fig. 2). The sediments from the northeast basin (NEB: including samples 92, 94, 105, 165, and 185) plot between the SPA and SC fields. However, sediments offshore from Indochina and from the Sunda Shelf cover a wide range of $^{87}Sr/^{86}Sr$ values (from 0.709 to 0.724), and are not able to be distinguished (Fig. 2). This zone is labeled as SW in Fig. 2 to represents the Sr isotopic range of the southwest SCS sediments, Sediments from the northern (sample S007) and southwest parts of the basin, and from the Nansha Islands mainly fall within the SW range, except for some samples from the southwest (samples S024, S031, and S043), which fall within the SC range (Fig. 2). Such regional differences in Sr and Nd isotope correlations suggest that Sr isotope values can be used in identifying the provenance of basic rocks around the Philippine Arc from continental sources, but are not able to identify those from different continental blocks.

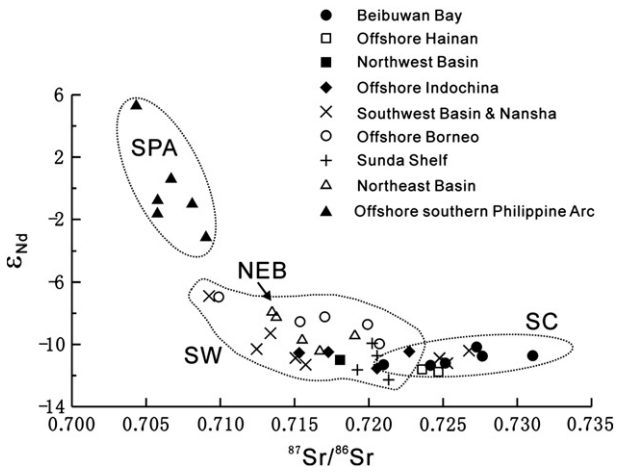

Fig. 2. Correlation between $^{87}Sr/^{86}Sr$ and ε_{Nd} of the South China Sea sediments. SC indicates the range of the sediment offshore from South China; NEB indicates those in the northeast basin; SW indicates those in the southwest SCS; and SPA indicates those offshore from the southern Philippine Arc.

4.3. Provenance analysis using element discrimination diagrams

Some elements are believed to be conservative during weathering, transportation, and sedimentary processes, making them useful for identifying the provenance of sediments and sedimentary rocks (Bhatia and Crook, 1986; Fralick and Kronberg, 1997). Rare earth elements (REEs) can be used to trace sedimentary provenance, including the Eu anomaly (Eu*) (Bhatia, 1985; McLennan, 1989), defined as $3\times Eu_N/(2\times Tb_N + Sm_N)$, where N indicates normalized by chondrite. The Eu* value of the SCS sediments varies from 0.5 to 0.8, except for samples S053 (0.45), 198 (0.90), and 254 (1.08) (Table 2). Fig. 3 shows the correlation between Eu* and Nd isotopes of these sediments. There only appears a moderate positive correlation between Eu* and Nd isotopes, with a correlation coefficient of 0.84 ($N=6$, $p<0.02$) for the sediments from the southern Philippine Arc, and no apparent correlation can be seen in the other sediments (Fig. 3). Moreover, no regional differences are apparent in Fig. 3, except for the sediments offshore from the southern Philippine Arc, and the Eu* values of sediments from different regions in the SCS show a degree of overlap. Consequently, the Eu anomaly is unsuitable as a provenance proxy for SCS sediments.

Among the commonly used elemental discrimination diagrams (Bhatia and Crook, 1986; Fralick and Kronberg, 1997), the La–Th–Sc diagram is one of the best to identify provenance for fine grain sediments for that these elements are generally random distributed and conservative during weathering, transportation, and sedimentary processes. Fig. 4 shows the La–Th–Sc diagram of the SCS sediments. It is interesting to see that zonal distributions are apparent for these sediments regionally assorted similar to that for Nd and Sr isotopes (Fig. 4). Because we have limited trace element data for sediments from the eastern part of the northern shelf and slope, Fig. 4 also shows data for sediments from ODP Site 1144, as reported by Shao et al. (2001). The sediments at ODP Site 1144 are derived mainly from the eastern South China Block, in particular from Taiwan Island (Shao et al., 2001), and they outline the field for the eastern South China Block and labeled as ESC (eastern South China) in Fig. 4. Sediments from the western margin of the SCS, including those from Beibuwan Bay, offshore Hainan Island, offshore Indochina and from the Sunda Shelf, show overlapping distributions in Fig. 4. They have a relatively low Sc and high La concentrations, and plot in the upper left of the diagram. This zone is labeled WM (west margin) and may represent the provenance of the western margin of the SCS. Sediments offshore from Borneo and from the Nansha Islands also overlap (Fig. 4), possessing low La and high Sc concentrations compared with sediments from the western margin, plotting below the WM field. This field is labeled SM to indicate the provenance of the southern margin of the SCS in Fig. 4. Sediments offshore from the southern Philippine Arc have a higher Sc concentration than those offshore from Borneo and Nansha Islands, plotting to the right of the SM field in Fig. 4. This zone is labeled SPA, indicating a southern

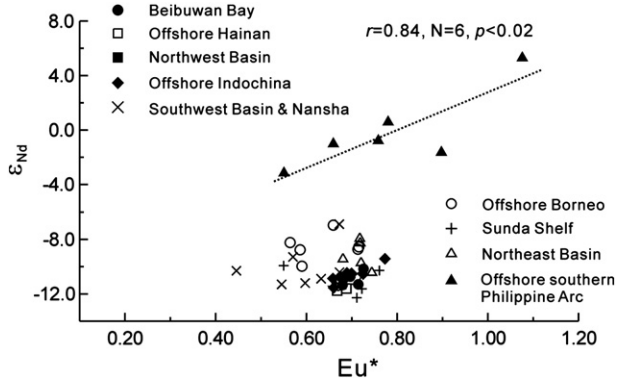

Fig. 3. Correlation between ε_{Nd} and Eu anomalies. The symbols are the same as in Fig. 2.

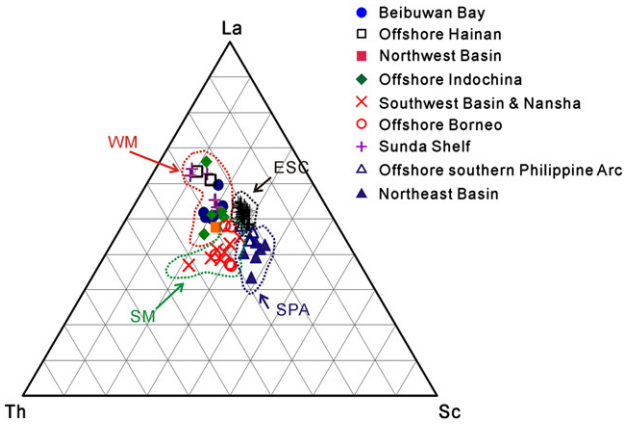

Fig. 4. La–Th–Sc discrimination diagram of the South China Sea sediments. The symbols are the same as in Fig. 2. Sediments at ODP Site 1144 are shown as thin crosses. The meanings of the abbreviations of the fields are as follows: ESC: the eastern South China; SPA: the southern Philippine Arc; WM: the west margins; and SM: the south margins.

Philippine Arc source. Sediments at ODP Site 1144 have higher Sc concentrations than those from the western margin of the SCS, and higher Th concentrations than those offshore from the southern Philippine Arc. In Fig. 4, these sediments, which plot to the right of the WM field and above the SPA field, are labeled ESC to indicate sources from the eastern South China Block. Sediments offshore from the northeast basin plot between ESC and SPA in Fig. 4, indicating a mixture of these two sources.

These zonal distributions of trace elements to some extent are similar to those for Nd isotopes. For example, sediments offshore from the southern Philippine Arc concentrate in the SPA field, corresponding to their highest ε_{Nd} values. Meanwhile, the sediments offshore from the northern Philippine Arc and from the northeast basin and lie between the ESC and SPA fields (Fig. 4), suggesting a mixing between sediments supplied from the eastern South China and the southern Philippine Arc. However, the other zonal distributions are different from those of the Nd isotopes. The sediments located offshore from Indochina and the Sunda Shelf have slightly higher ε_{Nd} values than those from Beibuwan Bay and offshore from Hainan Island, but they cannot be separated and all concentrate in the SM field of the La–Th–Sc discrimination diagram (Fig. 4). The distribution of sediments offshore from Borneo and those from Nansha Islands are overlapped, while the ε_{Nd} differences between them are significant.

The most valuable merit of the La–Th–Sc discrimination diagram lies in the distinct distribution of the SM and ESC fields. As shown in Fig. 4, sediments supplied from the eastern South China Block, represented by the ODP Site 1144 sediments, concentrate in the ESC field. Whereas the sediments supplied mainly from the western South China Block, represented by those from offshore of Hainan Island and Beibuwan Bay, concentrate in the SM filed. The two fields can be separated clearly due to the relative higher Sc concentrations of the sediments from the east than those from the west (Fig. 4). High Sc concentrations for the sediments from the east South China Block has formerly been recognized by Shao et al. (2009), but the differences can definitely be demonstrated in our La–Th–Sc discrimination diagram. Thus this diagram may potentially be used to identify sediments supplied from the eastern and western parts of the South China Block, which is difficult to achieve by Nd isotopes as mentioned above. It is therefore that coupled elemental discrimination diagrams and Nd isotopes may be more efficient in identifying the provenance of the SCS sediments.

4.3. Re-assessing the provenance of sediments at ODP Site 1148

ODP Site 1148 is the only scientific core in the SCS that extends to the late Oligocene, enabling an investigation of the opening and

evolution of the SCS (Wang et al., 2000). The changes in provenance of the sediments at ODP Site 1148 provide clues to the tectonic history of the opening and development of the SCS (Clift et al., 2002; Li et al., 2003). The Nd isotopes of clay minerals (<2 μm fraction) and bulk carbonate-free sediments have been analyzed by Clift et al. (2002) and Li et al. (2003), respectively. Both studies show a rapid ε_{Nd} drift at around 23.8 Ma, indicating a significant change in sediment provenance. A strong consensus exists regarding the provenance of sediments younger than 23.8 Ma (above 455 mcd), but the provenance of older sediments is debated (Clift et al., 2002; Li et al., 2003). Clift et al. (2002) explained the shift at 23.8 Ma in terms of the progressive headward erosion of river systems in South China, with the erosion changing from coastal South China to the interior of the South China Block at around this time. Li et al. (2003) suggested a sudden break in the sediment supply from the southern SCS at around 23.8 Ma due to the progressive enlargement of the SCS. These contrasting interpretations give rise to a problem for sediment supplying to the SCS that cannot be solved by Nd isotopes alone. Considering the applicability of both Nd isotopes and trace elements in tracing provenance, as indicated by the agreement in their regional distributions, we herein employ elemental discrimination diagrams, using data of sediments at ODP Site 1148, to further constrain the provenance of sediments in the SCS.

Fig. 5 shows data of the ODP Site 1148 sediments on a La–Th–Sc diagram (Fig. 5b). The Nd isotopic compositions reported by Clift et al. (2002) and Li et al. (2003) are also shown for comparison (Fig. 5a). The sediments can be divided into three groups according to their Nd isotopic compositions and physical characteristics. The first group comprises sediments above 455 mcd (younger than 23.8 Ma), which have more negative ε_{Nd} values. The second group consists of sediments beneath 477 mcd (older than 26 Ma), which have relatively high ε_{Nd} values, and the third group is intermediate between the first two groups, including the slump unit from 455 to 477 mcd. These three groups can be clearly distinguished in the La–Th–Sc diagram.

The sediments above 455 mcd at ODP Site 1148 generally plot in the ESC zone, which exactly overlaps those at ODP Site 1144. This result is consistent with their similar Nd isotopic compositions, which are comparable to those from the South China Block. Thus, these sediments were supplied from the South China Block, as indicated by Clift et al. (2002) and Li et al. (2003). Taiwan Island has been proposed as a potential source for sediments at ODP Site 1144 (Shao et al., 2001), but Taiwan could not be the source for Miocene sediments (>455 mcd) at ODP Site 1148, because the rapid uplift of Taiwan Island occurred during the Pliocene (after 6.5 Ma) (Huang et al., 2006). Taiwan was generally under seawater during the Miocene (Huang et al., 2006), receiving sediment mainly from the eastern South China Block. It is therefore likely that the Miocene and younger sediments of the main mountain range on Taiwan Island and of ODP Site 1148 were derived from the same source, resulting in similar ε_{Nd} values and overlapped distributions in the La–Th–Sc diagram (Fig. 5b). The eastern South China Block (Cathaysia sources) was possibly the main provenance of these sediments.

None of the sediments at >455 mcd at ODP Site 1148 fall within the WM field in Fig. 5b, As the main of the Pearl River system, in particular its upper reaches are located in the Yangtze Block (Fig. 1). It is therefore sediments supplied from the upper reaches of the Pearl River system may have similar geochemical characteristics to those from offshore Hainan Island and Beibuwan Bay, which are concentrated in the SM field in the La–Th–Sc discrimination diagram. The separate distribution of the >455 mcd sediments at ODP Site 1148 away from the WM field in Fig. 5b suggests that sediments supplied from the upper reaches of the Pearl River system did not significantly contribute to the region around ODP Site 1148 after 23.8 Ma. This result does not support the progressive headward erosion hypothesis, which states that materials eroded from the interior of the South China Block by river systems represent the bulk of the sediment at ODP Site 1148 after 23.8 Ma (Clift et al., 2002; Shao et al., 2008). It is therefore the sediments at >455 mcd at ODP Site 1148 are mainly supplied from the eastern South China Block (Cathaysia sources).

The sediments beneath 477 mcd at ODP Site 1148 plot mainly in the SPA field in Fig. 5b. The Philippine Arc, however, is not their source because the islands of the Philippine Arc were located far from ODP Site 1148, separated by the proto-South China Sea (Hall, 2002). Also, these sediments do not plot in the ESC or WM fields (Fig. 5b), and their Nd isotopic compositions are significant higher than those of the >455 mcd sediments, both for bulk sediments (Li et al., 2003) and clay minerals (Clift et al., 2002) (also shown in Fig. 5a). Moreover, their ε_{Nd} values are generally more positive than those supplied from the modern South China Block (see Fig. 1). Giving that ODP Site 1148 is next to the South China Block, sediments eroded from coastal South China should contribute the main of the sediments at this site, as suggested by Clift et al. (2002). Different geochemical compositions of the sediments erode from the South China Block before 26 Ma from those after 23.8 Ma appear to account for the differences between the sediments at <477 mcd and those at >455 mcd at ODP Site 1148. There emerge a large amount of Cretaceous granitoids in the coastal South China, with the youngest ages of about 90 Ma (Li,

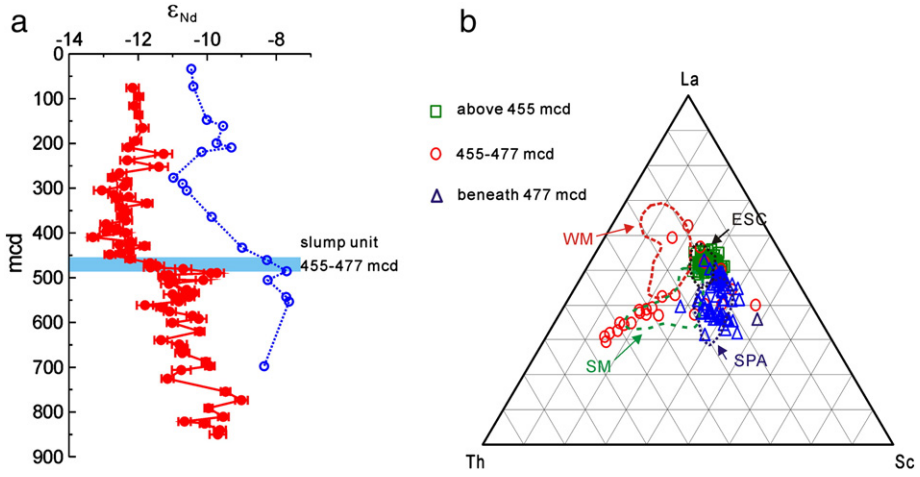

Fig. 5. Variations of ε_{Nd} values and La–Th–Sc discrimination diagram of the sediments at ODP Site 1148; a) ε_{Nd} profile: open circles indicate the <2 μm fraction (Clift et al., 2002) and solid circles indicate bulk sediments; b) La–Th–Sc discrimination diagram. The fields and their abbreviations are the same as those in Fig. 4.

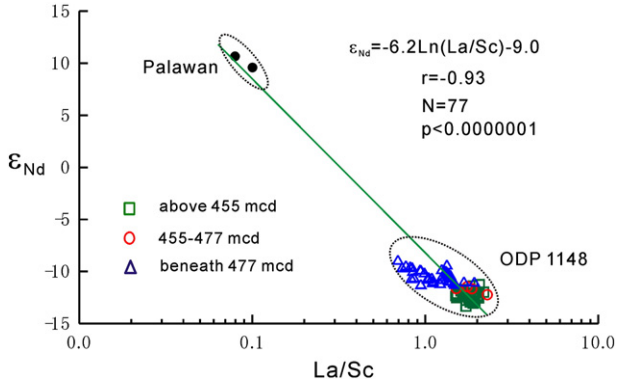

Fig. 6. Correlation between ε_{Nd} and La/Sc ratios of sediments at ODP Site 1148 and basalts of the North Palawan Continental Terrane. Symbols are the same as Fig. 5b.

2000). Giving that granitoids are generally formed at depth of >5 km, there may be a huge cover on these granitoids during the late Cretaceous and to the early Cenozoic. These materials may possibly contribute to the sediments in the ancient South China Sea. If they have different geochemical composition from those erode from granitoids, which account for much of the modern sediments, this may interpret the changes in the sediments at ODP 1148.

However, it is difficult to identify such materials erode from the covers on the granitoids in South China. The Mesozoic and the early Cenozoic sediments in Taiwan Island (Huang et al., 2006) and the old sediments (before Oligocene) from oil-field wells in basins along coastal South China may give hints for them Shao et al. (2008). However, their detailed geochemical compositions are limited, and no evaluations could be made currently. The other places that may retain these materials could be the North Palawan Continental Terrane and the Reed Bank or the so-called Dangerous Grounds, including the North Palawan Continental Terrane, the Reed Bank and the whole Nansha Islands (Spratley Islands) in the new tectonic model (Clift et al., 2008). Current location of the North Palawan Continental Terrane is next to the southern Philippine Arc, and the Reed Bank is located to its west (Fig. 1). They were all located along the coastal of South China before Eocene (>40 Ma) (Lee and Lawver, 1994; Clift et al., 2008). Even though geochemical details of these blocks are not known currently, they may possibly contain materials similar to those covered on the granitoids in South China, and retain their geochemical compositions. Moreover, these two blocks may have contributed to the sediments offshore from the southern Philippine Arc due to their close locations, and influence the geochemical compositions of the sediments offshore from the southern Philippine Arc. More importantly, these two blocks were located close to ODP Site 1148 till the late Oligocene (Lee and Lawver, 1994; Hall, 2002; Clift et al., 2008). They may have contributed significantly to the sediments at ODP Site 1148, explaining why the sediments older than 23.8 Ma plot within the SPA field in the La–Th–Sc diagram.

It is worth noting that the ε_{Nd} values of the sediments offshore from the southern Philippine Arc are much more positive (−3.7 to +5.3) than those at ODP Site 1148 before 26 Ma (−9.8 to −11.4). This difference may reflect the input of weathering products of volcanic rocks, mainly basalt and andesite with high ε_{Nd} (Goldstein and Jacobsen, 1988), from the southern Philippine Arc. The weathering products of volcanic rocks may also have contributed to sediments at ODP Site before 23.8 Ma, as the SCS oceanic crust was actively extending during this period (Briais et al., 1993), possibly enhancing the supply of volcanic material from oceanic crust and surrounding volcanic activity. This possibility is also indicated by the extremely high smectite content in the fine fraction (<2 μm) of these sediments. Smectite accounts for more than 40% of the fine fraction in these sediments, with a maximum of 90% (Clift et al., 2002; Tang et al., 2004). The chemical weathering of continental rocks generally does not produce such a high smectite content in weathering products; consequently, the chemical weathering of volcanic rocks in seawater is proposed as the most likely process (Thiry, 2000). The enhanced input of volcanic material that accompanied the extension of SCS oceanic crust provided abundant material for smectite production by weathering under the influence of seawater. This proposal is further supported by the La/Sc–ε_{Nd} diagram (Fig. 6), which shows that the post-23.8 Ma sediments at ODP Site 1148 have the most negative ε_{Nd} values and high La/Sc ratios, and those older than 26 Ma have higher ε_{Nd} values and lower La/Sc ratios. Basalts from the North Palawan Continental Terrane have the highest ε_{Nd} values and the lowest La/Sc ratios (Tu et al., 1992). The La/Sc and ε_{Nd} of the ODP Site 1148 sediments and the North Palawan Continental Terrane basalts show a rough mixing trend in Fig. 6, indicating that weathering products from volcanic rocks also contributed to the sediments at ODP Site 1148 before 26 Ma.

The rapid change in sediments from 477 mcd to 455 mcd at ODP Site 1148 indicates that sediment supplies change from those with SPA characteristics before 26 Ma to those with ESC characteristics. This provenance change was very quick, lasting for less than 3 Ma (Li et al., 2005). It is unlikely that the materials covered on the granitoids in South China exactly run out in ~3 Ma during that period for that weathering on continents is generally a slow process. We herein propose that this provenance change may attribute from the southwards drift of the North Palawan Continental Terrane and Reed Bank along with the opening of the SCS. Giving that these two blocks were next to ODP Site 1148 till 30 Ma (Lee and Lawver, 1994; Hall, 2002; Clift et al., 2008), they may have contributed significantly to the sediments at ODP Site 1148 before Oligocene. Along with the enlargement of the SCS basin after 30 Ma, the distance from these two blocks to ODP Site 1148 was increasing. Meanwhile, global sea-level was increasing in the late Oligocene (Haq et al., 1987). When the SCS basin was large enough and the water depth was deep enough at ~26 Ma, sediment supply to the region around ODP Site 1148 from the two blocks margin ceased, resulting in a rapid change in sediment provenance at ODP Site 1148 at 26–23.8 Ma.

The sediments of the slump unit from 455 mcd to 477 mcd fall within a wide range in the La–Th–Sc diagram. Some samples plot in the ESC, SPA, and even WM fields, but the majority of data points fall within the SM field (Fig. 5b). The dispersing distribution is consistent with the rapid change in provenance during this period. As detrital components of the sediments were not well deposited at this section, and biogenic and authigenic materials composed of the main (Li et al., 2005), their source regions are still difficult to be identified.

5. Summary

We reported on the mineralogy, major and trace elements, and neodymium and strontium isotopes of surface sediments in the SCS, and assessed their applicability in tracing the provenance of the sediments. The change in provenance of sediments at ODP Site 1148 since the late Oligocene was re-assessed based on Nd isotopes and element discrimination diagrams. The main results of this study are as follows.

1) The sediments in the SCS are dominated by rock-forming minerals; clay mineral content is generally less than 50%. None of the minerals shows a clear zonal distribution that can be used to identify their sources. Thus, mineralogical composition alone is not useful for tracing the provenance of bulk sediments in the SCS.
2) The Nd isotopic compositions of these sediments show clear zonal distributions. Sediments on the northern shelves and slopes (offshore from South China) have the most negative ε_{Nd} values, from −13.0 to −10.7, while sediments offshore from Indochina are slightly more positive, from −10.7 to −9.4. The Nd isotopic

compositions of sediments offshore from Borneo are even higher, with ε_{Nd} values from −8.8 to −7.0, and the sediments offshore from the southern Philippine Arc have the most positive ε_{Nd} values, from −3.7 to +5.3. This ε_{Nd} distribution agrees well with the Nd isotopic compositions of the sediments supplied by river systems that drained to the corresponding regions, and the ε_{Nd} values of sediments located between these regions show mixing trends. This result indicates that Nd isotopic compositions are an adequate proxy for tracing the provenance of SCS sediments.

Coupled with Nd isotopes, Sr isotopic compositions can be used to identify the provenance of SCS sediments. Sediments offshore from South China have the highest $^{87}Sr/^{86}Sr$ (0.7210–0.7310) and lowest ε_{Nd} (−10.2 to −13.0) values, while sediments offshore from the southern Philippine Arc have the lowest $^{87}Sr/^{86}Sr$ (0.7043–0.7090) and highest ε_{Nd} (−3.7 to +5.3) values, meaning that they are easily identified. However, the sediments offshore from Indochina and offshore from Borneo cannot be identified based on Sr isotopic compositions because they show overlapping $^{87}Sr/^{86}Sr$ ratios.

3) The zonal distribution of SCS sediments is also apparent in the La–Th–Sc diagram. Sediments offshore from the western South China Block, offshore from Indochina, and from the Sunda Shelf overlap in the diagram, representing the western margin of the SCS. Sediments from the eastern South China Block, offshore from the southern Philippine Arc, and offshore from the Borneo plot in distinct fields in the La–Th–Sc diagram. This distribution is generally consistent with the distribution of Nd isotopes and is likely to be controlled by the sediment source. Thus, the La–Th–Sc discrimination diagram is a reliable indicator of the provenance of SCS sediments.
4) Based on Nd isotopes and the La–Th–Sc discrimination diagram, we re-assessed the provenance change recorded by sediments at ODP Site 1148 since the late Oligocene. The sediments above 455 mcd at this site show similar ε_{Nd} values to those of the South China Block, and generally plot in the eastern South China Block field in a La–Th–Sc diagram, suggesting that these sediments were supplied mainly from the eastern South China Block after 23.8 Ma. The sediments beneath 477 mcd have higher ε_{Nd} values and generally plot in the southern Philippine Arc field. Materials covered on the late Mesozoic granitoids in coastal South China may contribute to them. These materials possibly retains in the North Palawan Continental Terrane and served as an important source for the sediments at ODP Site 1148 for that the North Palawan Continental Terrane, which is now located in the southern Philippine Arc, but during the late Oligocene was located next to ODP Site 1148. Volcanic material associated with extension of the SCS oceanic crust may also have contributed to the sediments before 26 Ma. Sediments deposited during the transition period (477 to 455 mcd) show dispersing distribution in the La–Th–Sc diagram, and their provenances are still difficult to be identified. The rapid change in provenance at ODP Site 1148 at 26–23.8 Ma was probably caused by a sudden cessation of sediment supply from the North Palawan Continental Terrane, due to the southward drift of the North Palawan Continental Terrane that accompanied the extension of the SCS oceanic crust at this time, because the North Palawan Continental Terrane became too distant to supply sediment to ODP Site 1148.

Acknowledgements

The authors thank Dr. Tu Xianglin of the State Key Laboratory of Isotope Geochemistry, Guangzhou Institute of Geochemistry (GIG), Chinese Academy of Sciences for his help in trace element measurements, and South China Sea Institute of Oceanography, CAS for providing the NS series sediment samples. Discussions on geology of South China with Prof. Li Xianhua of the Institute of Geology and Geophysics, CAS, and Prof. Wang Qiang of the GIG, CAS are helpful. The critical and constructive comments of the two anonymous reviews help to improve the manuscript. Thanks also go to Dr. Aaron Stallard for helps in proofs the English of this manuscript. This work was supported by the Knowledge Innovation Project of the Chinese Academy of Sciences (grant KZCX2-YW-138), National Basic Research Program of the Chinese Ministry of Science and Technology (grant 2009CB421206), and the National Natural Science Foundation of China (grant 40973008, 91128212). This is contribution No. IS-1529 from GIGCAS.

References

Asahara, Y., Tanaka, T., Kamioka, H., Nishimura, A., Yamazaki, T., 1999. Provenance of the north Pacific sediments and process of source material transport as derived from Rb–Sr isotopic systematics. Chemical Geology 158 (3–4), 271–291.
Barr, S.M., MacDonald, A.S., 1981. Geochemistry and geo-chronology of late Cenozoic basalts of Southeast Asia. Geological Society of America Bulletin (Part II) 92, 1069–1142.
Bhatia, M.R., 1985. Rare earth element geochemistry of Australian Paleozoic graywackes and mudrocks: provenance and tectonic control. Sedimentary Geology 45, 97–113.
Bhatia, M.R., Crook, K.A.W., 1986. Trace element characteristics of graywackes and tectonic discrimination of sedimentary basins. Contributions to Mineralogy and Petrology 92, 181–193.
Briais, A., Patriat, P., Tapponnier, P., 1993. Updated interpretation of magnetic-anomalies and sea-floor spreading stages in the South China Sea — implications for the tertiary tectonics of Southeast-Asia. Journal of Geophysical Research-Solid Earth 98 (B4), 6299–6328.
Chen, C.H., Lee, T.P., 1990. A Nd–Sr isotopic study on river sediments of Taiwan. Proceedings of the Geological Society of China 33, 339–350.
Chen, C.H., Shieh, Y.N., Lee, T.P., Mertzman, S.A., 1990. Nd–Sr–O isotopic evidence for source contamination and an unusual mantle component under Luzon Arc. Geochimica et Cosmochimica Acta 54 (9), 2473–2483.
Clift, P., Il Lee, J., Clark, M.K., Blusztajn, J., 2002. Erosional response of South China to arc rifting and monsoonal strengthening; a record from the South China Sea. Marine Geology 184 (3–4), 207–226.
Clift, P.D., Blusztajn, J., Duc, N.A., 2006a. Large-scale drainage capture and surface uplift in eastern Tibet–W China before 24 Ma inferred from sediments of the Hanoi Basin, Vietnam. Geophysics Research Letters 33, L19403, http://dx.doi.org/10.1029/2006GL027772.
Clift, P.D., Carter, A., Campbell, I.H., Pringle, M., Hodges, K.V., Lap, N.V., Allen, C.M., 2006b. Thermochronology of mineral grains in the Song Hong and Mekong Rivers, Vietnam. Geochemistry, Geophysics, Geosystems 7, Q10005, http://dx.doi.org/10.1029/2006GC001336.
Clift, P.D., Lee, G.H., Nguyen, A.D., Barckhausen, U., Hoang, V.L., Sun, Z., 2008. Seismic evidence for a Dangerous Grounds mini-plate: no extrusion origin for the South China Sea. Tectonics 27, TC3008, http://dx.doi.org/10.1029/2007TC002216.
Derry, L.A., France-Lanord, C., 1996. Neogene Himalayan weathering history and river Sr-87/Sr-86: impact on the marine Sr record. Earth and Planetary Science Letters 142 (1–2), 59–74.
Fedo, C.M., Sircombe, K.N., Rainbird, R.H., 2003. Detrtial zircon analysis of the sedimentary record. In: Hanchar, J.M., Hoskin, P.W.O. (Eds.), Zircon: Reviews in Mineralogy and Geochemistry, 53, pp. 277–303.
Fralick, P.W., Kronberg, B.I., 1997. Geochemical discrimination of elastic sedimentary rock sources. Sedimentary Geology 113 (1–2), 111–124.
Ge, T., 2009. The characteristics of Mineralogy and element geochemistry of the red weathering crusts in Weizhou Island and Xieyan Island, Beibu Gulf. Thesis for Master's Degree at the Graduate University of Chinese Academy of Sciences.
Goldstein, S.J., Jacobsen, S.B., 1988. Nd and Sr isotopic systematics of River water suspended material — implications for crustal evolution. Earth and Planetary Science Letters 87 (3), 249–265.
Goldstein, S.L., O'Nions, R.K., Hamilton, P.J., 1984. A Sm–Nd isotopic study of atmospheric dusts and particulates from river systems. Earth and Planetary Science Letters 70, 221–236.
Graham, I.J., Glasby, G.P., Churchman, G.J., 1997. Provenance of the detrital component of deep-sea sediments from the SW Pacific Ocean based on mineralogy, geochemistry and Sr isotopic composition. Marine Geology 140 (1–2), 75–96.
Gui, X.T., Yu, J.S., Li, X.H., Chen, S.M., 1994. Sr–O isotopic composition of sediments in the Nnsha Sea Area and paleo-environment. Chinese Science Bulletin 39, 124–129.
Hall, R., 2002. Cenozoic geological and plate tectonic evolution of SE Asia and the SW Pacific: computer-based reconstructions, model and animations. Journal of Asian Earth Sciences 20 (4), 353–431.
Haq, B.U., Hardenbol, J., Vail, P.R., 1987. Chronology of fluctuating sea levels since the Triassic. Science 235, 1156–1167.
Hemming, S.R., van de Flierdt, T., Goldstein, S.L., Franzese, A.M., Roy, M., Gastineau, G., Landrot, G., 2007. Strontium isotope tracing of terrigenous sediment dispersal in the Antarctic Circumpolar Current: implications for constraining frontal positions. Geochemistry, Geophysics, Geosystems 8, Q06N13, http://dx.doi.org/10.1029/2006GC001441.
Huang, Z.G., Cai, F.X., Han, Z.Y., Chen, J.H., Zong, Y.Q., Lin, X.D., 1993. Quaternary Volcano in Leizhou Peninsula and Hainan Island. Science Press.

Huang, C.Y., Yuan, P.B., Tsao, S.J., 2006. Temporal and spatial records of active arc-continent collision in Taiwan: a synthesis. Geological Society of America Bulletin 118, 274–288.
Lee, T.Y., Lawver, L.A., 1994. Cenozoic Plate reconstruction of the South China Sea Region. Tectonophysics 235 (1–2), 149–180.
Li, X.H., 2000. Cretaceous magmatism and lithospheric extension in Southeast China. Journal of Asian Earth Sciences 18, 293–305.
Li, X.H., Liu, Y., Tu, X.L., Hu, G.Q., Zeng, W., 2002. Precise determination of chemical compositions in silicate rocks using ICP-AES and ICP-MS. A comparative study of sample digestion techniques of alkali fusion and acid dissolution. Geochimica 31 (3), 289–294 (in Chinese with English abstract).
Li, X.H., Wei, G.J., Shao, L., Liu, Y., Liang, X.R., Jian, Z.M., Sun, M., Wang, P.X., 2003. Geochemical and Nd isotopic variations in sediments of the South China Sea: a response to Cenozoic tectonism in SE Asia. Earth and Planetary Science Letters 211 (3–4), 207–220.
Li, Q.Y., Jian, Z.M., Su, X., 2005. Late Oligocene rapid transformations in the South China Sea. Marine Micropaleontology 54, 5–25.
Liang, X.R., Wei, G.J., Li, X.H., Liu, Y., 2003. Precise measurement of $^{143}Nd/^{144}Nd$ and Sm/Nd ratios using multiple-collectors inductively coupled plasma-mass spectrometry (MC-ICPMS). Geochimica 32 (1), 91–96 (in Chinese with English abstract).
Liu, Y., Liu, H.C., Li, X.H., 1996. Simultaneous and precise determination of 40 trace elements in rock samples using ICP-MS. Geochimica 25 (6), 552–558 (in Chinese with English abstract).
Liu, Z.F., Colin, C., Huang, W., Le, K.P., Tong, S.Q., Chen, Z., Trentesaux, A., 2007. Climatic and tectonic controls on weathering in south China and Indochina Peninsula: clay mineralogical and geochemical investigations from the Pearl, Red, and Mekong drainage basins. Geochemistry, Geophysics, Geosystems 8, Q05005, http://dx.doi.org/10.1029/2006GC001490.
Liu, Z.F., Tuo, S.T., Colin, C., Liu, J.T., Huang, C.Y., Selvaraj, K., Chen, C.T.A., Zhao, Y.L., Siringan, F.P., Boulay, S., Chen, Z., 2008. Detrital fine-grained sediment contribution from Taiwan to the northern South China Sea and its relation to regional ocean circulation. Marine Geology 255 (3–4), 149–155.
Ma, J.L., Wei, G.J., Xu, Y.G., Long, W.G., 2010. Variations of Sr-Nd-Hf isotopic systematics in basalt during intensive weathering. Chemical Geology 269, 376–385.
McCulloch, M.T., Wasserburg, G.J., 1978. Sm–Nd and Rb–Sr chronology of continental crust formation. Science 200, 1003–1011.
McDermott, F., Defant, M.J., Hawkesworth, C.J., Maury, R.C., Joron, J.L., 1993. Isotope and trace-element evidence for 3 component mixing in the genesis of the North Luzon Arc Lavas (Philippines). Contributions to Mineralogy and Petrology 113 (1), 9–23.
McDermott, F., Delfin, F.G., Defant, M.J., Turner, S., Maury, R., 2005. The petrogenesis of volcanics from Mt. Bulusan and Mt. Mayon in the Bicol arc, the Philippines. Contributions to Mineralogy and Petrology 150 (6), 652–670.
McLennan, S.M., 1989. Rare earth elements in sedimentary rocks: influence of provenance and sedimentary processes. In: Lipin, B.R., McKay, G.A. (Eds.), Geochemistry and mineralogy of rare earth elements: Reviews in Mineralogy, 21, pp. 169–200.
McLennan, S.M., Hemming, S., McDaniel, D.K., Hanson, G.N., 1993. Geochemical approaches to sedimentation, provenance, and tectonics. Geological Society of America Special Paper 284, 21–40.
Miller, R.G., O'Nions, R.K., 1984. The provenance and crustal residence ages of British sediments in relation to palaeogeographic reconstructions. Earth and Planetary Science Letters 68, 459–470.
Miller, R.G., O'Nions, R.K., 1985. Source of Precambrian chemical and clastic sediments. Nature 314, 325–330.
Shao, L., Li, X.H., Wei, G.J., Liu, Y., Fang, D.Y., 2001. Provenance of a prominent sediment drift on the northern slope of the South China Sea. Chinese Science Bulletin 44 (10), 919–925.
Shao, L., Pang, X., Qiao, P.J., Chen, C.M., Li, Q.Y., Miao, W.L., 2008. Sedimentary filling of the Pearl River Mouth Basin and its response to the evolution of the Pearl River. Acta Sedimentologica Sinica 26, 179–185.
Shao, L., Qiao, P.J., Pang, X., Wei, G.J., Li, Q.Y., Miao, W.L., Li, A., 2009. Nd isotopic variations and its implications in the recent sediments from the northern South China Sea. Chinese Science Bulletin 54 (2), 311–317.
Shi, X.F., Yan, Q.S., Wang, K.S., 2007. Mineral provinces and material provenance of the surficial sediments near the Zhongsha Islands in the South China Sea. Acta Oceanologica Sinica 26 (1), 66–76.
Tang, S., Shao, L., Zhao, Q.H., 2004. Characteristics of clay mineral in South China Sea since Oligocene and its significance. Acta Sedimentologica Sinica 22, 337–342.
Thiry, M., 2000. Palaeoclimatic interpretation of clay minerals in marine deposits: an outlook from the continental origin. Earth-Science Reviews 49, 201–221.
Tu, K., Flower, M.F.J., Carlson, R.W., Xie, G., Chen, C.-Y., Zhang, M., 1992. Magmatism in the South China Basin, 1. Isotopic and trace-element evidence for an endogenous Dupal mantle component. Chemical Geology 97, 47–63.
Vroon, P.Z., Vanbergen, M.J., Klaver, G.J., White, W.M., 1995. Strontium, neodymium, and lead isotopic and trace-element signatures of the East Indonesian sediments — provenance and implications for Banda Arc Magma Genesis. Geochimica et Cosmochimica Acta 59 (12), 2573–2598.
Wang, P., Prell, W.L., Blum, P., 2000. Proc. ODP, Init. Repts. 184 [CD-ROM]Ocean Drilling Program, Texas A&M University, College Station TX77845-9547, USA.
Wang, Y.J., Fan, W.M., Guo, F., Peng, T.P., Li, C.W., 2003. Geochemistry of Mesozoic mafic rocks adjacent to the Chenzhou-Linwu fault, South China: implications for the lithospheric boundary between the Yangtze and Cathaysia blocks. International Geology Review 45 (3), 263–286.
Wei, G.J., Liang, X.R., Li, X.H., Liu, Y., 2002. Precise measurement of Sr isotopic composition of liquid and solid base using (LP)MC-ICPMS. Geochimica 31 (3), 295–299 (in Chinese with English abstract).
Wei, G.J., Liu, Y., Tu, X.L., Liang, X.R., Li, X.H., 2004. Separation of Sr, Sm and Nd in mineral and rock samples using selective specific resins (in Chinese with English abstract). Rock and Mineral Analysis 23, 11–14.
Winter, B.L., Johnson, C.M., Clark, D.L., 1997. Strontium, neodymium, and lead isotope variations of authigenic and silicate sediment components from the Late Cenozoic Arctic Ocean: implications for sediment provenance and the source of trace metals in seawater. Geochimica et Cosmochimica Acta 61 (19), 4181–4200.
Wu, W.H., Xu, S.J., Yang, J.D., Yin, H.W., Lu, H.Y., Zhang, K.J., 2010. Isotopic characteristics of river sediments on the Tibetan Plateau. Chemical Geology 269, 406–413.
Yan, Y., Xia, B., Lin, G., Carter, A., Hu, X.Q., Cui, X.J., Liu, B.M., Yan, P., Song, Z.J., 2007. Geochemical and Nd isotope composition of detrital sediments on the north margin of the South China Sea: provenance and tectonic implications. Sedimentology 54 (1), 1–17.
Yang, S.Y., Yim, W.W.S., Huang, G.Q., 2008. Geochemical composition of inner shelf quaternary sediments in the northern South China Sea with implications for provenance discrimination and paleoenvironmental reconstruction. Global and Planetary Change 60 (3–4), 207–221.
Zhang, Z.J., Wang, Y.H., 2007. Crustal structure and contact relationship revealed from deep seismic sounding data in South China. Physics of the Earth and Planetary Interiors 165, 114–126.